STRUCTURAL CHEMISTRY

ISSN 2053-2296

Formation of extended polyiodides at large cation templates

Alexander J. Blake,[a]* Carlo Castellano,[b] Vito Lippolis,[c] Enrico Podda[d] and Martin Schröder[e]

[a]School of Chemistry, University of Nottingham, University Park, Nottingham, NG7 2RD, United Kingdom, [b]Dipartimento di Chimica, Università degli Studi di Milano, Via Golgi 19, Milano, 20133, Italy, [c]Dipartimento di Scienze Chimiche e Geologiche, Università degli Studi di Cagliari, S.S. 554 Bivio per Sestu, Monserrato (CA), 09042, Italy, [d]Centre for Research University Services (CeSAR), Università degli Studi di Cagliari, S.S. 554 Bivio per Sestu, Monserrato (CA), 09042, Italy, and [e]Department of Chemistry, The University of Manchester, Manchester, M139PL, United Kingdom. *Correspondence e-mail: alexanderjohnblake@outlook.com

Received 9 April 2024
Accepted 7 May 2024

Edited by I. Oswald, University of Strathclyde, United Kingdom

Keywords: crystal structure; mixed-donor macrocycles; [2.2.2]cryptand; palladium(II) complexes; diiodine; polyiodides; FT-Raman spectroscopy.

CCDC references: 2353843; 2353842

Supporting information: this article has supporting information at journals.iucr.org/c

By studying the structures of (μ-1,4,10,13-tetrathia-7,16-diazacyclooctadecane)-bis[iodidopalladium(II)] diiodide penta(diiodine), $[Pd_2I_2(C_{12}H_{26}N_2S_4)](I)_2{\cdot}5I_2$ or $[Pd_2I_2([18]aneN_2S_4)](I)_2{\cdot}(I_2)_5$, and 4,7,13,16,21,24-hexaoxa-1,10-diazoniabicyclo[8.8.8]hexacosane triiodide iodide hemipenta(diiodine) dichloromethane monosolvate, $C_{18}H_{38}N_2O_6^{2+}{\cdot}I_3^-{\cdot}I^-{\cdot}2.5I_2{\cdot}CH_2Cl_2$ or $[H_2([2.2.2]cryptand)](I_3)(I)(I_2)_{2.5}{\cdot}CH_2Cl_2$, we confirm the structural variety of extended polyiodides achievable upon changing the shape, charge and dimensions of the cation template, by altering the synthetic strategy adopted and/or the experimental conditions. Although it is still often difficult to characterize discrete $[I_{2m+n}]^{n-}$ polyiodides higher than I_3^- on the basis of structural parameters, such as I—I bond distances, FT–Raman spectroscopy appears to identify them as aggregates of I_2, I^- and (symmetric or slightly asymmetric) I_3^- building blocks linked by I···I interactions of varying strengths. However, because FT–Raman spectroscopy carries no information about the topological features of extended polyiodides, the two techniques should therefore be applied in combination to enhance the analysis of this kind of compounds.

1. Introduction

Among extended anionic inorganic frameworks, the formation of polyhalides (Sonnenberg *et al.*, 2020; Aragoni *et al.*, 2003, 2022) and, in particular, polyiodides represents a remarkable example of supramolecular self-assembly (Blake *et al.*, 1998*c*; Svensson *et al.*, 2003), and it continues to capture the interest of many researchers in the field (Savastano, 2021; Savastano *et al.*, 2022; Horn *et al.*, 2003*a*,*b*; Aragoni *et al.*, 2004, 2023*a*) due to the richness of its unpredictable and puzzling structural chemistry, and interesting applicative possibilities (Paulsson *et al.*, 2004; Yin *et al.*, 2012; Fei *et al.*, 2015). Iodine and iodides together tend to catenate (Arca *et al.*, 1999; Garau *et al.*, 2022) *via* the combination of (Lewis acidic) I_2 with (Lewis basic) I^-/I_3^- building blocks (Ciancaleoni *et al.*, 2016). This affords extended arrays exhibiting a range of topologies, and these are highly dependent on the size, shape and charge of the countercation acting as a template. Some polyiodides are present in the crystal structure as discrete aggregates, but frequently they form extended networks in which the identification of the basic repeat unit of general formula $[I_n(I_2)_m]^{n-}$ or $[I_{2m+n}]^{n-}$ (n, $m > 0$) can become arbitrary. Consequently, they are better described as aggregates of I_2, I^- and I_3^-, held together by I···I interactions of varying strengths, from rather strong (*ca* 3.3 Å) to fairly weak, up to the van der Waals contact distance (*ca*

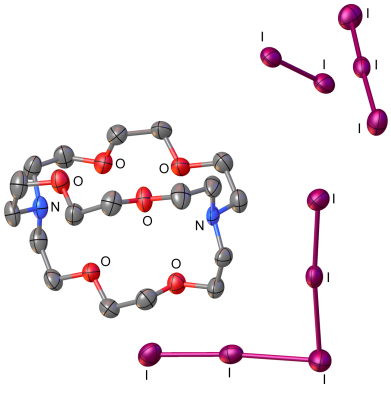

Table 1
Experimental details.

For both structures: Z = 4. Experiments were carried out with Mo $K\alpha$ radiation.

	(I)	(II)
Crystal data		
Chemical formula	$[Pd_2I_2(C_{12}H_{26}N_2S_4)](I)_2{\cdot}5I_2$	$C_{18}H_{38}N_2O_6^{2+}{\cdot}I_3^-{\cdot}I^-{\cdot}2.5I_2{\cdot}CH_2Cl_2$
M_r	2315.99	1605.53
Crystal system, space group	Monoclinic, $C2/c$	Monoclinic, $P2_1/n$
Temperature (K)	220	293
a, b, c (Å)	21.609 (4), 8.198 (3), 24.151 (3)	13.831 (2), 14.820 (2), 20.266 (3)
β (°)	100.170 (13)	96.70 (1)
V (Å^3)	4211.1 (18)	4125.6 (10)
μ (mm^{-1})	11.33	6.92
Crystal size (mm)	0.26 × 0.14 × 0.13	0.2 × 0.15 × 0.11
Data collection		
Diffractometer	STOE STADI4 4-circle	Bruker APEXII CCD
Absorption correction	Integration (*REDU4*; Stoe & Cie, 1996)	Empirical (using intensity measurements) (*SADABS*; Bruker, 2001)
T_{min}, T_{max}	0.222, 0.306	0.569, 1.000
No. of measured, independent and observed [$I > 2\sigma(I)$] reflections	4584, 3715, 3059	30347, 8100, 5518
R_{int}	0.029	0.047
(sin $\theta/\lambda)_{max}$ (Å^{-1})	0.595	0.617
Refinement		
$R[F^2 > 2\sigma(F^2)]$, $wR(F^2)$, S	0.051, 0.136, 1.08	0.033, 0.088, 1.00
No. of reflections	3715	8100
No. of parameters	163	349
H-atom treatment	H-atom parameters constrained	H atoms treated by a mixture of independent and constrained refinement
$\Delta\rho_{max}$, $\Delta\rho_{min}$ (e Å^{-3})	1.35, −1.62	1.37, −1.20

Computer programs: *STADI4* (Stoe & Cie, 1996), *SAINT* (Bruker, 2001), *REDU4* (Stoe & Cie, 1996), *SHELXS97* (Sheldrick, 1997), *SHELXT2018* (Sheldrick, 2015*a*), *SHELXL2018* (Sheldrick, 2015*b*) and *OLEX2* (Dolomanov *et al.*, 2009).

4 Å). Our interest in this field has been mainly focused on the use of metal complexes of macrocyclic ligands (mainly thioether crowns) as templating cations for controlling the self-assembly of extended polyiodide arrays (Blake *et al.*, 1996, 1998*a*,*b*). These complex cations are relatively chemically inert and their shape, size and charge can be changed readily, thus providing cationic templates for different targeted polyiodide topologies. Furthermore, we have also been interested in the reactivity of macrocyclic ligands with I_2 and inter-halogens IX (X = Br and Cl) to better understand the structural nature of the resulting products (Blake *et al.*, 1997). The formation of polyiodide networks featuring spirals, belts, ribbons, sheets and cages as their structural motifs has been achieved either by reacting the PF_6^- or BF_4^- salts of the complex cation

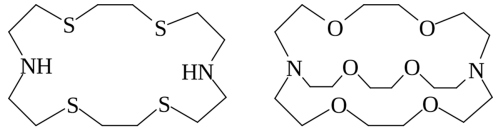

[18]aneN$_2$S$_4$ [2.2.2]cryptand

Scheme 1

templates with an excess of I_2 in a single phase, or by addition of an NaI/I_2 mixture in a single phase, the preferred polyiodide being formed *via* self-assembly. As a further example of the versatility of this synthetic approach to the formation of multidimensional polyiodide networks, we report here the use of the metal complex $[Pd_2Cl_2([18]aneN_2S_4)](PF_6)_2$ ([18]aneN$_2$S$_4$ is 1,4,10,13-tetrathia-7,16-diazacyclooctadecane; see Scheme 1) and the neutral [2.2.2]cryptand (4,7,13,16,21,24-hexaoxa-1,10-diazabicyclo[8.8.8]hexacosane) (Scheme 1) as templates in the reaction with I_2.

2. Experimental

2.1. Materials and methods

All starting materials, including [18]aneN$_2$S$_4$ and [2.2.2]-cryptand, and solvents, were obtained from Aldrich or Merck and were used without further purification. $[Pd_2Cl_2([18]aneN_2S_4)](PF_6)_2$ was prepared according to the literature (Blake *et al.*, 1990). Microanalytical data were obtained on a Fisons EA 1108 CHNS-O instrument operating at 1000 °C. FT–Raman spectra (resolution 4 cm^{-1}) were recorded on a Bruker RF100FTR spectrometer fitted with an indium–gallium–arsenide detector operating at room temperature with an excitation wavelength of 1064 nm (Nd:YAG laser). No sample decomposition was observed during the experiments at the power level of the laser source used between 20 and 40 mW. The values in parentheses next to the values represent the intensities of the peaks relative to the strongest, which is taken to be equal to 10.

2.2. Synthesis and crystallization

2.2.1. Synthesis of (I). To a solution of $[Pd_2Cl_2([18]aneN_2S_4)](PF_6)_2$ (17.1 mg, 0.019 mmol) in MeCN (4 ml) was added a solution of I_2 (17.7 mg, 0.070 mmol) in MeCN (4 ml).

No precipitate formed upon mixing, but dark-brown prismatic crystals of title compound (I) (Scheme 2) formed after several days by slow evaporation of the solvent from the reaction mixture. These were isolated from the mother liquor and washed with diethyl ether (8.4 mg, 36.3% yield). Elemental analysis found [calculated (%) for $C_6H_{13}I_7NPdS_2$]: C 6.28 (6.22), H 1.15 (1.13), N 1.24 (1.21), S 5.52 (5.54). FT–Raman (range 500–50 cm^{-1}): ν(I–I) 169.7 (10).

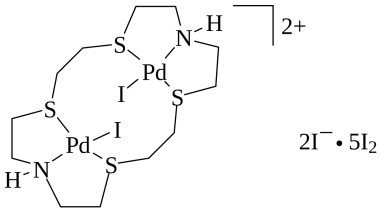

$[Pd_2I_2([18]aneN_2S_4)](I)_2\cdot(I_2)_5$

(I)

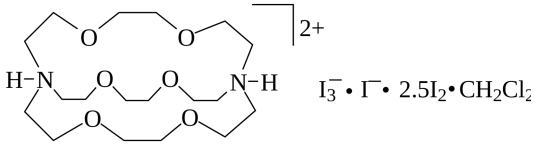

$[H_2([2.2.2]cryptand)](I_3)(I)(I_2)_{2.5}\cdot CH_2Cl_2$

(II)

Scheme 2

2.2.2. Synthesis of (II). To a solution of [2.2.2]cryptand (20 mg, 0.053 mmol) in CH_2Cl_2 (4 ml) was added a solution of I_2 (53.8 mg, 0.212 mmol) in CH_2Cl_2 (4 ml). A dark-brown microcrystalline precipitate corresponding to the formulation of title compound (II) (Scheme 2) formed immediately. This was isolated by filtration and washed with diethyl ether (58.5 mg, 77.3% yield). Elemental analysis found [calculated (%) for $C_{19}H_{40}Cl_2I_9N_2O_6$]: C 14.25 (14.21), H 2.47 (2.51), N 1.80 (1.75). FT–Raman (range 500–50 cm^{-1}): ν(I–I) 167.40 (10), 149.8 (6), 106.1 (5). Dark-brown prismatic single crystals suitable for X-ray diffraction analysis were grown from a solution of the obtained solid in MeCN by slow evaporation of the solvent.

2.3. Refinement of X-ray crystal structures

Crystal data, data collection and structure refinement details are summarized in Table 1. H atoms were placed geometrically and refined isotropically riding on their parent C atoms, with $U_{iso}(H) = 1.2U_{eq}(C)$. For (II), H atoms bonded to quaternary N atoms could be located from the difference Fourier map and their positions were refined freely. *OLEX2* (Dolomanov *et al.*, 2009) was used both as the graphical interface for the structural investigation and for the preparation of the figures.

3. Results and discussion

3.1. Synthesis and crystal structures

Previously, we have reported the crystal structures of $[Pd_2Cl_2([18]aneN_2S_4)](I_3)_2$ (Blake *at al.*, 1998*c*,*d*) and $[Pd_2Cl_2([18]aneN_2S_4)]_{1.5}(I_5)(I_3)_2$ (Blake *et al.*, 1998*a*,*c*) obtained from the reaction in MeCN of $[Pd_2Cl_2([18]aneN_2S_4)](PF_6)_2$ with $^nBu_4NI$ and I_2 in 1:2:2 and 1:2:4 molar ratios, respectively. In the former compound, dinuclear palladium(II) complexes are linked *via* Pd···I contacts into $\cdots I_3^-\cdots I_3^-\cdots I_3^-\cdots$ sinusoidal chains. In $[Pd_2Cl_2([18]aneN_2S_4)]_{1.5}(I_5)(I_3)_2$, $[Pd_2Cl_2([18]aneN_2S_4)]^{2+}$ cations are held together by N—H···Cl hydrogen bonds and occupy channels formed within the self-assembled three-dimensional (3D) polyiodide network. This network is made up of offset layers of stacked poly-I_3^- moieties (including those I_3^- belonging to the I_5^- units), featuring fused 14- and 24-membered rings interwoven by I_8^{2-} units ($I_5^-\cdots I_3^-$). We sought to attempt also the direct reaction of $[Pd_2Cl_2([18]aneN_2S_4)](PF_6)_2$ with I_2 in the absence of pre-formed I^- (see §2.2.1) and, surprisingly, this afforded a different compound corresponding to the formulation $[Pd_2I_2([18]aneN_2S_4)]I_{12}$, as deep-red column-shaped crystals. A single-crystal X-ray structure determination (see Table 1 for crystal data) showed an asymmetric unit consisting of half a $[Pd_2I_2([18]aneN_2S_4)]^{2+}$ dication, one iodide anion interacting with two crystallographically-independent I_2 molecules, and an additional half-occupied I_2 molecule disordered across a twofold axis parallel to the *b* axis. One of the two I atoms is located on a glide plane, thus defining an overall stoichiometry of $[Pd_2I_2([18]aneN_2S_4)](I)_2\cdot(I_2)_5$, (I), for the obtained salt. The complete dication is generated through an inversion centre and features the hexadentate macrocycle binding to the two

Table 2
Selected geometric parameters (Å, °).

$[Pd_2I_2([18]aneN_2S_4)](I)_2\cdot(I_2)_5$, (I)			
Pd—I	2.5722 (14)	S7—C8	1.816 (12)
Pd—N1	2.076 (9)	C8—C9	1.511 (16)
Pd—S4	2.314 (3)	I—I^{ii}	3.545 (2)
Pd—$S7^i$	2.313 (3)	I1—I2	2.7899 (15)
N1—C2	1.459 (15)	I2—I3	3.1214 (16)
N1—$C9^i$	1.489 (16)	I3—I4	3.205 (2)
C2—C3	1.514 (17)	I4—I5	2.7644 (16)
C3—S4	1.809 (11)	I3—I6	3.351 (3)
S4—C5	1.838 (10)	I6—I7	2.771 (4)
C5—C6	1.507 (15)	I7—$I3^{iii}$	3.432 (3)
C6—S7	1.796 (10)		
N1—Pd—S4	86.8 (3)	$S7^i$—Pd—I	92.20 (8)
N1—Pd—$S7^i$	87.7 (3)	$S7^i$—Pd—S4	173.88 (11)
S4—Pd—I	93.57 (8)		
$[H_2([2.2.2]cryptand)](I_3)(I)(I_2)_{2.5}\cdot CH_2Cl_2$, (II)			
I3—I2	2.9799 (8)	O1—C2	1.402 (8)
I3—I4	2.8629 (8)	O1—C3	1.422 (8)
I6—I5	2.8015 (8)	O2—C4	1.426 (8)
I6—I7	3.0952 (8)	O2—C5	1.430 (8)
I8—I9	2.8001 (8)	O3—C9	1.415 (8)
I8—I7	3.0940 (9)	O3—C8	1.431 (8)
I1—$I1^{iv}$	2.7595 (11)	O4—C11	1.421 (8)
N1—C1	1.495 (9)	O4—C10	1.428 (8)
N1—C12	1.493 (8)	O5—C17	1.421 (8)
N1—C13	1.507 (8)	O5—C16	1.403 (8)
N2—C6	1.500 (8)	O6—C15	1.408 (8)
N2—C7	1.495 (8)	O6—C14	1.429 (8)
N2—C18	1.506 (8)		
I4—I3—I2	176.54 (2)	I9—I8—I7	175.52 (2)
I5—I6—I7	173.63 (2)	I8—I7—I6	89.70 (2)

Symmetry codes: (i) $-x+\frac{3}{2}, -y+\frac{1}{2}, -z+1$; (ii) $-x+\frac{3}{2}, -y-\frac{1}{2}, -z+1$; (iii) $-x+1, y+1, -z+\frac{1}{2}$; (iv) $-x+2, -y+1, -z$.

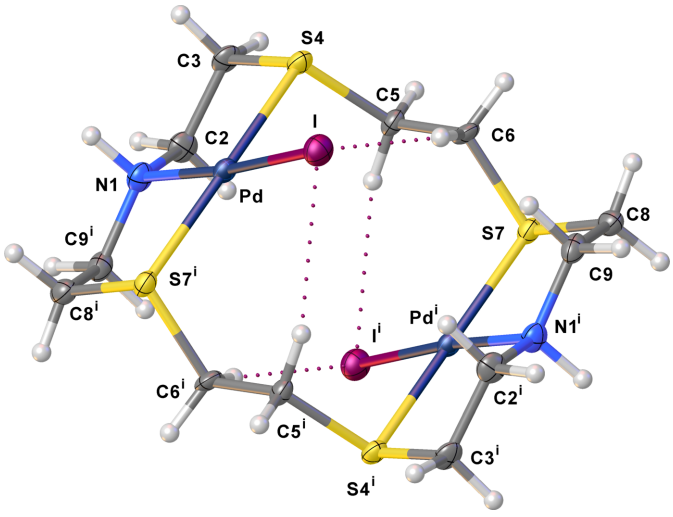

Figure 1
View of the dication in (I), showing the atom-numbering scheme adopted. Displacement ellipsoids are drawn at the 50% probability level. Intramolecular C—H···I hydrogen bonds: C6···I = 3.779 (11), H6*A*···I = 2.84, C5^{i}···I = 3.755 (10), H5*A*···I = 2.80 Å, C6—H6*A*···I = 162 and C5—H5*A*···I^{i} = 161°. [Symmetry code: (i) $-x+\frac{3}{2}, -y+\frac{1}{2}, -z+1$.]

metal centres *via* NS_2 coordination. A distorted square-planar coordination geometry at each Pd^{II} metal ion is completed by coordinated iodide anions that have replaced the chloride ions (Fig. 1) in the starting material upon reaction with I_2 (see Table 2 for selected geometric parameters).

In (I), the Pd—N [Pd—N1 = 2.076 (9) Å] and Pd—S [Pd—S4 = 2.314 (3) and Pd—S7^{i} = 2.313 (3) Å; symmetry code: (i) $-x+\frac{3}{2}, -y+\frac{1}{2}, -z+1$] distances are very close to those observed in previously reported $[Pd_2Cl_2([18]aneN_2S_4)]^{2+}$ dications (Blake *et al.*, 1990, 1998*a*,*c*,*d*), while the Pd—I bond distance [2.5722 (14) Å] is significantly longer than the Pd—Cl distances [2.305 (4)–2.374 (1) Å]. As with the $[Pd_2Cl_2([18]aneN_2S_4)]^{2+}$ dications reported previously, the dications in (I) adopt a stepped conformation. Interestingly, in $[Pd_2Cl_2([18]aneN_2S_4)]_{1.5}(I_5)(I_3)_2$ (Blake *et al.*, 1998*a*,*c*), the dications are linked pairwise by hydrogen bonds between the (N)H and Cl atoms to form extended chains. The $[Pd_2I_2([18]aneN_2S_4)]^{2+}$ dications in (I) are linked by intermolecular I···I contacts of 3.545 (2) Å to form chains running parallel to the *b* axis (Fig. 2). In both compounds, the complex dications feature intermolecular interactions of the type C—H···*X* (*X* = Cl and I) (see Figs. 1 and 2).

The polyiodide network in (I) can also be regarded as comprising I_{12}^{2-} anions (Fig. 3) built up by $[(I^-)_2{\cdot}(I_2)_5]$ adducts formed by interaction of the disordered I_2 molecules (I6—I7) [2.771 (4) Å] and 'V-shaped' I_5^- of the type $[(I^-){\cdot}(I_2)_2]$ with the iodide anion (I3) interacting with two crystallographically-independent I_2 molecules [I1—I2 and I4—I5: I1—I2 = 2.7899 (15), I2···I3 = 3.1214 (16), I4—I5 = 2.7644 (16), I3···I4 = 3.205 (2) Å, I1—I2···I3 = 173.23 (5), I3···I4—I5 = 173.60 (5) and I2···I3···I4 = 95.36 (4)°].

Each component of the disordered and half-occupied I_2 molecule interacts at both I atoms with the iodide atom (I3) of the I_5^- moiety *via* I···I interactions of 3.351 (3) (I3···I6) and 3.432 (3) Å [I7···I3^{iv}; symmetry code: (iv) $-x+1, y+1, -z+\frac{1}{2}$]. This gives rise to two I_{12}^{2-} anions in the structure, which are symmetry-related by a screw axis parallel to the *b* axis and a glide plane (the same symmetry elements that relate the two disorder components of the half-occupied I6—I7 diiodine molecule) (Fig. 3).

I_{12}^{2-} of the same orientation (blue or green in Fig. 3) interact with each other *via* I···I interactions of 3.625 (2) [I1···I7^{vi}; symmetry code: (vi) $x-\frac{1}{2}, y-\frac{1}{2}, z$] and 3.800 (2) Å [I6···I5^{vii}; symmetry code: (vii) $-x+1, -y+1, -z+1$] (Fig. 4) to give one-dimensional (1D) tubes of fused pseudo-cubic cavities defined by 8- and 14-membered polyiodide rings (Fig. 4). Two differently-oriented 1D tubes of this type therefore co-exist at 50% occupancy in the crystal structure, depending on the orientation of the generating I_{12}^{2-} units; one type is approximately perpendicular and the other approximately parallel to the [110] direction (blue and green, respectively, in Fig. 5).

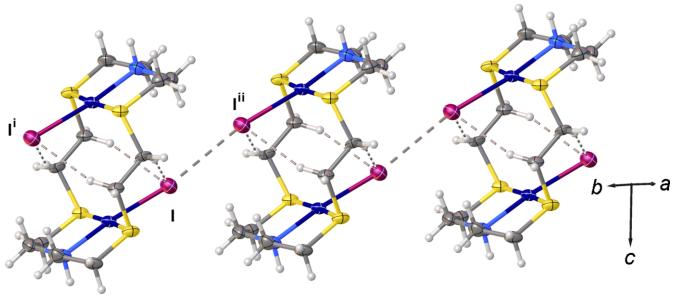

Figure 2
View of a chain of interacting $[Pd_2I_2([18]aneN_2S_4)]^{2+}$ dications found in the crystal structure of (I). The dications are arranged into chains *via* I···I interactions of 3.545 (2) Å running along the *b* axis. [Symmetry codes: (i) $-x+\frac{3}{2}, -y+\frac{1}{2}, -z+1$; (ii) $-x+\frac{3}{2}, -y-\frac{1}{2}, -z+1$.]

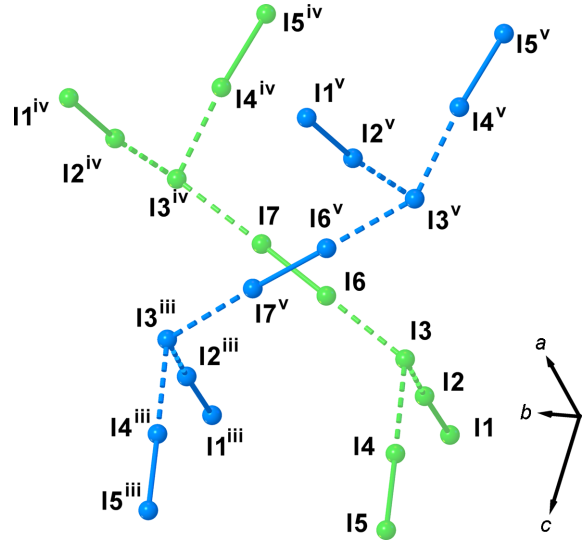

Figure 3
View of the two symmetry-related I_{12}^{2-} anions in (I) formed by the interaction of the two components of the disordered I_2 molecules with two 'V-shaped' I_5^- moieties of the type $[(I^-){\cdot}(I_2)_2]$. [Symmetry codes: (iii) *x*, *y* + 1, *z*; (iv) $-x+1, y+1, -z+\frac{1}{2}$; (v) $-x+1, y, -z+\frac{1}{2}$.]

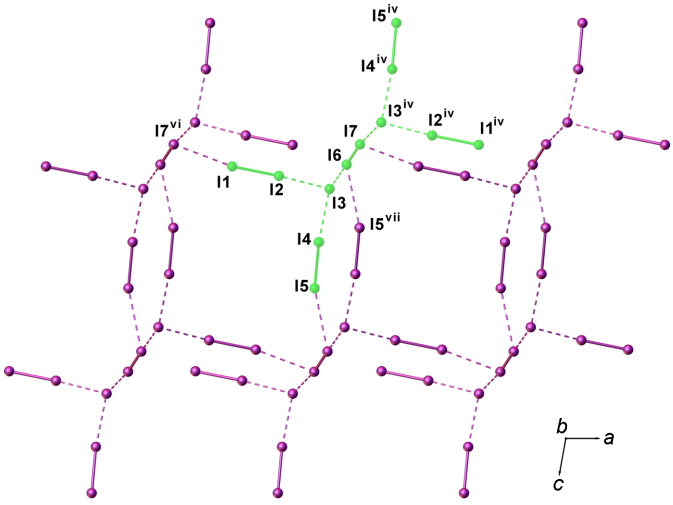

Figure 4
View along the *b* axis of one of the two 1D polyiodide tubes in (I) formed *via* $I_{12}^{2-}\cdots I_{12}^{2-}$ interactions involving I_{12}^{2-} anions of the same orientation (in this case, I_{12}^{2-} is the component depicted in green as in Fig. 3). [Symmetry codes: (iv) $-x+1, y+1, -z+\frac{1}{2}$; (vi) $x-\frac{1}{2}, y-\frac{1}{2}, z$; (vii) $-x+1, -y+1, -z+1$.]

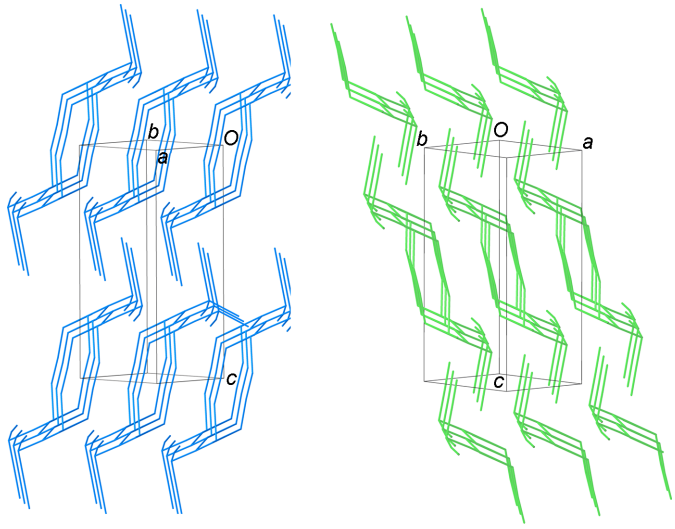

Figure 5
View of the two differently-oriented polyiodide 1D tubes of interacting I_{12}^{2-} units co-existing at 50% occupancy in the crystal structure of (I). Colours are consistent with those in Fig. 3 for the differently-oriented I_{12}^{2-} units generating the two 1D polyiodides tubes.

Chains of $[Pd_2I_2([18]aneN_2S_4)]^{2+}$ complex dications (Fig. 2) run parallel to the *b* axis crossing adjacent 1D polyiodide tubes through the pseudo-cubic cavities (Fig. 6). It is interesting to note that, as the I7 atom of the disordered I_2 molecule lies on a glide plane, the resulting ratio between the two components is imposed by symmetry and the maximum occupancy possible is 0.5. As a consequence, the ratio between the two types of tubes described above remains constant in the crystal structure and cannot vary between different crystals. That said, a unique crystal packing is observed in the crystal structure of (I) featuring the two sets of tubes formed by fused pseudo-cubic boxes (see above) running parallel (green) and perpendicular (blue) to the [110] direction, alternatively layered along the *c* axis [Figs. 6(*b*) and 6(*c*)].

To illustrate further the importance of the shape, charge and dimensions of the template cation in the polyiodide network assembly, we treated the macropolycyclic ligand [2.2.2]cryptand (Scheme 1) with I_2 in a 1:4 molar ratio in CH_2Cl_2. Upon

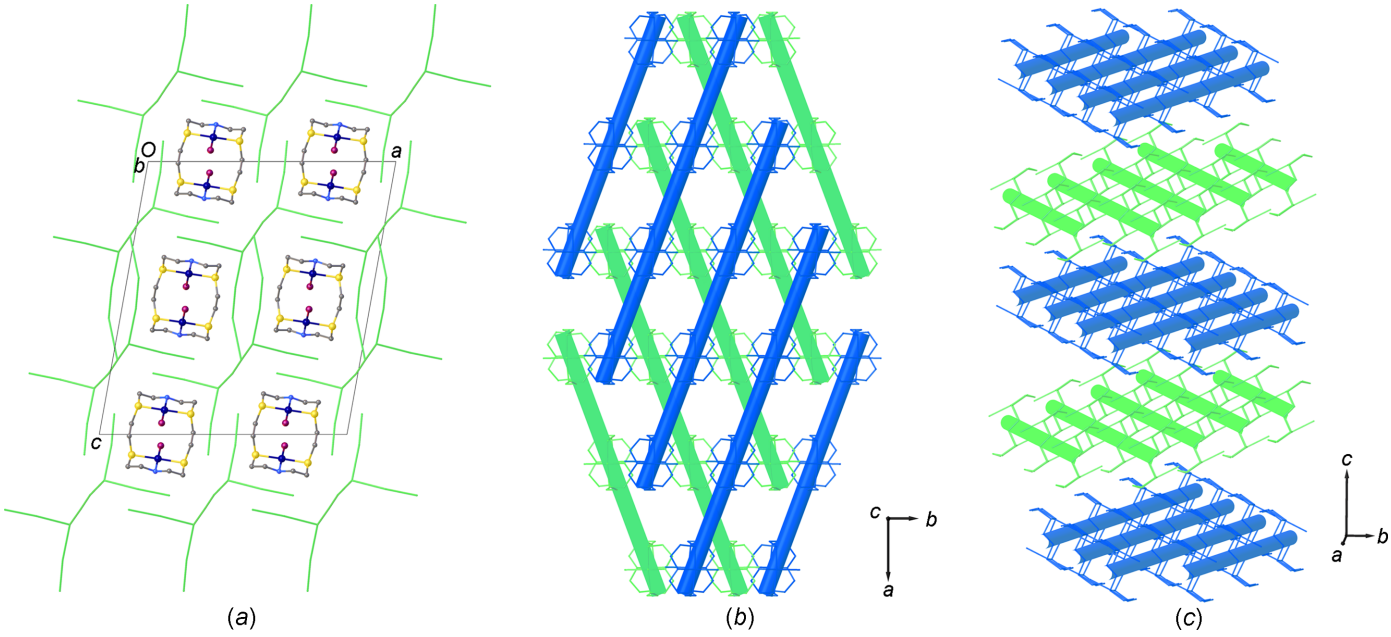

Figure 6
(*a*) View along the *b* axis of the crystal packing in (I), showing the relative positions between the 1D polyiodide tubes and the chains of $[Pd_2I_2([18]aneN_2S_4)]^{2+}$ complex dications. The polyiodide network is also portrayed in parts (*b*) and (*c*) as blue and green tubes according to Fig. 3, and cations are coloured according to the type of tubes they cross.

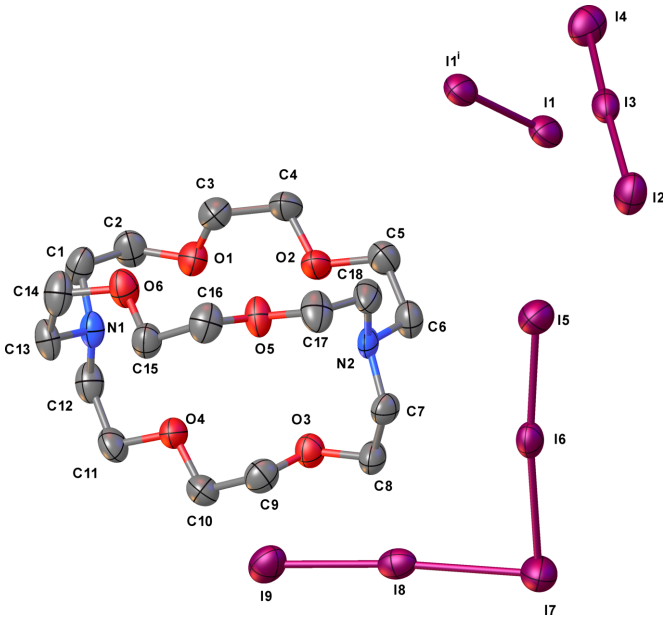

Figure 7
The crystal structure of (II), showing the numbering scheme adopted. Displacement ellipsoids are drawn at the 50% probability level. H atoms and the cocrystallized CH_2Cl_2 molecules are not shown. [Symmetry code: (i) $-x+2, -y+1, -z$.]

slow evaporation of the solvent at room temperature, dark prismatic crystals formed corresponding to the formulation $[H_2([2.2.2]\text{cryptand})]I_9\cdot CH_2Cl_2$, (II). An X-ray crystal structure determination (see Table 1 for crystal data) confirmed the presence of an asymmetric unit consisting of an $[H_2([2.2.2]\text{-cryptand})]^{2+}$ dication in which both tertiary N atoms of the starting macropolycyclic ligand are protonated (Fig. 7). Half an I_2 molecule [I1—I1^{i} = 2.7595 (11) Å; symmetry code: (i) $-x+2, -y+1, -z$], an asymmetric triiodide [I2—I3—I4: I2—I3 = 2.9799 (8) and I3—I4 = 2.8629 (8) Å], a 'V-shaped' pentaiodide consisting of an iodide anion (I7) interacting with two diiodine molecules $[(I^-)\cdot(I_2)_2]$ (I5—I6 and I8—I9) [I5—I6 = 2.8015 (8), I8—I9 = 2.8001 (8), I6—I7 = 3.0952 (8) and I7—I8 = 3.0940 (9) Å] and a cocrystallized CH_2Cl_2 solvent molecule define the $[H_2([2.2.2]\text{cryptand})](I_3)(I)(I_2)_{2.5}\cdot CH_2Cl_2$ (II) stoichiometry for the obtained polyiodide salt (see Table 2 for selected geometric parameters).

In (II), all three diiodine molecules are slightly elongated with respect to the I—I distance found in the crystal structure of orthorhombic I_2 [2.715 (6) Å] (Blake *et al.*, 1998*b*). Each I1 atom interacts with an asymmetric triiodide unit at the I2 atom to afford a 'Z-shaped' I_8^{2-} dianion [I1···I2 = = 3.4123 (9) Å] that can be regarded as an $I_3^-\cdot I_2\cdot I_3^-$ $[(I_3^-)_2\cdot(I_2)]$ complex (Savastano *et al.*, 2022). Additional longer contacts of 3.907 (1) Å, still within the sum of the van der Waals radii for iodine, between each I1 atom and the terminal iodine (I5) of a pentaiodide moiety, lead to an overall discrete 'grasshopper-shaped' I_{18}^{4-} polyiodide. This can be envisaged as an $[(I_8^{2-})\cdot(I_5^-)_2]$ with a long contact between the I_8^{2-} anion and the two I_5^- moieties or, in terms of fundamental building blocks, as an $[(I^-)_2\cdot(I_3^-)_2\cdot(I_2)_5]$ adduct (Fig. 8). I_{18}^{4-} polyiodides are quite rare in the literature: in $[Co(12C4)_2]_2(I_{18})$ (12C4 is 12-crown-4), a unique central planar I_9^- $[(I^-)\cdot(I_2)_4]$ is attached to four triiodides at I···I distances of 3.240 (4)–3.478 (4) Å, and the $[(I_9^-)(I_3^-)_4]$ units are connected *via* two bridging I_3^- to form polymeric chains of $I_{18}^{4-} = [(I_9^-)(I_3^-)_{2/1}\text{-}(I_3^-)_{2/2}]$ (Fiolka *et al.* 2011); in $[SnI_2(\text{mbit})_2](I_3)_2\cdot\frac{2}{3}I_2$ [mbit is 1,1′-bis(3-methyl-4-imidazoline-2-thione)methane], two I_8^{2-} dianions of the type $I_2\cdot I^-\cdot I_2\cdot I^-\cdot I_2$ $[(I^-)_2\cdot(I_2)_3]$ and related through an inversion centre are linked to each other at the iodide atoms by a bridging disordered I_2 molecule *via* non-negligible I···I interactions of 3.55 (1) Å (Bigoli *et al.*, 1998).

The discrete I_{18}^{4-} polyiodide units are located side-by-side and interdigitated along the [101] direction, with $[H_2([2.2.2]\text{-cryptand})]^{2+}$ dications sitting in the resulting voids (Fig. 9).

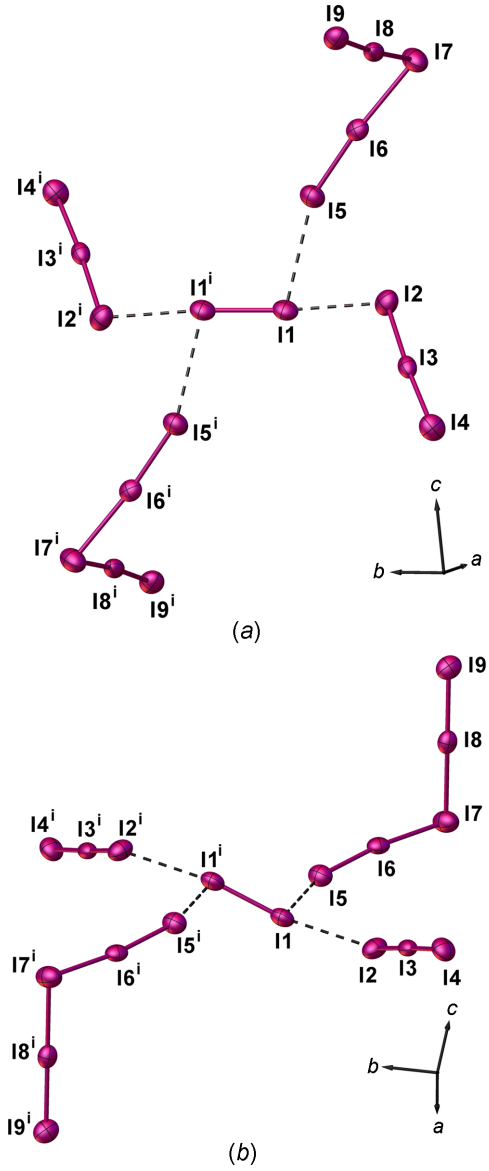

Figure 8
(*a*)/(*b*) Views of the I_{18}^{4-} polyiodide in (II) formed by interaction of a central diiodine molecule with two I_3^- and two I_5^- $[(I^-)\cdot(I_2)_2]$ species, showing the numbering scheme adopted. Displacement ellipsoids are drawn at the 50% probability level. [Symmetry code: (i) $-x+2, -y+1, -z$.]

3.2. FT–Raman spectroscopy

Despite the high number of extended polyiodides that have been structurally characterized, and the associated crystal structure data available, the assignment of higher molecular polyiodides (higher than I_3^-) with their own distinctive structural features is still a matter of debate (Savastano *et al.*, 2022). The reductionist approach whereby higher polyiodides are considered as aggregates of I_2, I^- and I_3^- held together by I···I interactions of varying strengths, from rather strong (up to *ca* 3.3–3.4 Å) (covalent interactions) to fairly weak (up to the van der Waals contact distance, *ca* 4 Å) (supramolecular interactions), is still the most reasonable and least arbitrary. On the basis of structural data, all known higher discrete polyiodides can be regarded, therefore, as weak or medium-weak adducts of the type $[(I^-)_{n-y}\cdot(I_3^-)_y\cdot(I_2)_{m-y}] \equiv [I_{2m+n}]^{n-}$ ($n, m > 0$), whose geometrical and topological features can be very different and often unpredictable (Arca *et al.* 2006). This way of considering higher polyiodides from a structural point of view is strongly supported by spectroscopic evidence. In particular, FT–Raman spectroscopy confirms that extended polyiodides do not have distinctive vibrational properties other than those of perturbed (slightly elongated) I_2 molecules and symmetric/slightly asymmetric I_3^-. Perturbed I_2 molecules are characterized by only one strong band in the range 180–140 cm^{-1} in the FT–Raman spectrum, the wavenumber depending on the extent of the I···I elongation; for linear and symmetric I_3^-, only the Raman-active symmetric stretch (ν_1) occurs near 110 cm^{-1}, while the antisymmetric stretch (ν_3) and the bending deformation (ν_2) are only IR-active (Aragoni *et al.*, 2023*b*). The latter two modes also become Raman-active for slightly asymmetric I_3^- and they are found near 134 (ν_3) and 80 cm^{-1} (ν_2), having medium and medium–weak intensities, respectively. Highly asymmetric I_3^- ions show only one band in their FT–Raman spectra in the range 180–140 cm^{-1}, so that they should be regarded as weak $(I^-)\cdot I_2$ adducts. To date, FT–Raman spectra of polyiodides of the general formula $[I_{2m+n}]^{n-}$ show peaks in the low wavenumber region with either one strong peak in the range 180–140 cm^{-1} or the characteristic peaks due to both perturbed I_2 and symmetric/slightly asymmetric I_3^-. They would therefore be better described as $[(I^-)_n\cdot(I_2)_m]$ or $[(I^-)_{n-y}\cdot(I_3^-)_y\cdot(I_2)_{m-y}]$ ($n > y \neq 0$)/$[(I_3^-)_n\cdot(I_2)_{m-n}]$ ($n = y \neq 0$) systems. The polyiodides here described are no exception. The FT–Raman spectrum of (I) features only a strong and broad peak centred at 169 cm^{-1} indicative of the presence of differently perturbed I_2 molecules (Fig. S1 in the supporting information). The FT–Raman spectrum of (II) is shown in Fig. 10. The two peaks at about 167 and 150 cm^{-1} can be assigned to the stretching vibration of the two differently elongated I_2 molecules I5—I6/I6—I7

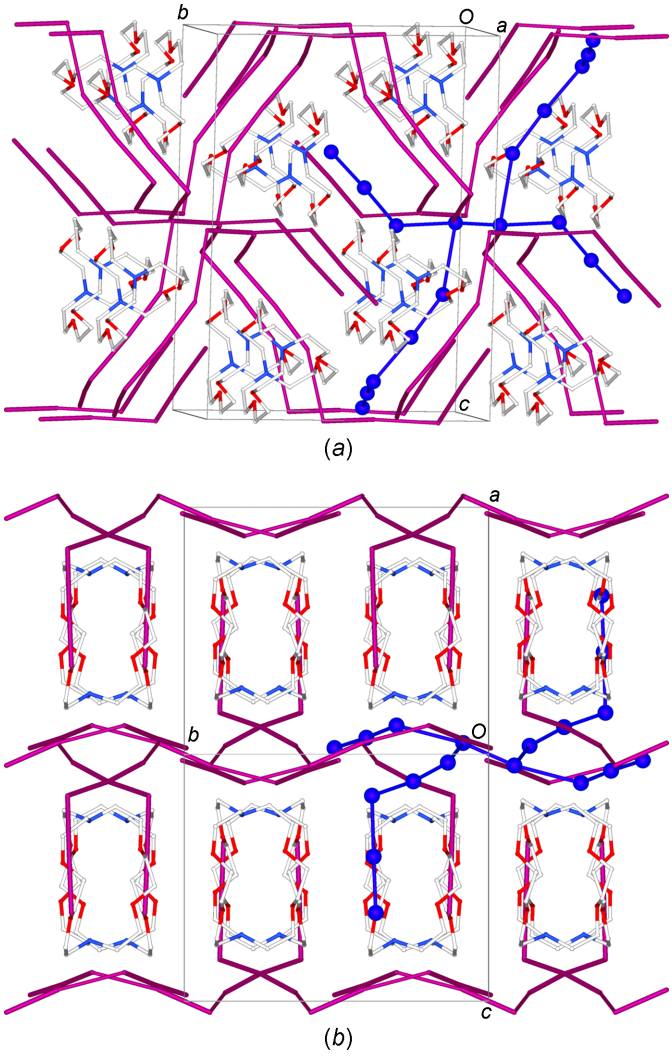

Figure 9
Views along approximately (*a*) the *a* axis and (*b*) the [101] direction of the crystal packing in (II). The blue colour and the ball-and-stick representation have been used for one of the discrete I_{18}^{4-} polyiodide units to better highlight its atomic connectivity in the crystal packing. H atoms and the cocrystallized CH_2Cl_2 molecules are not shown.

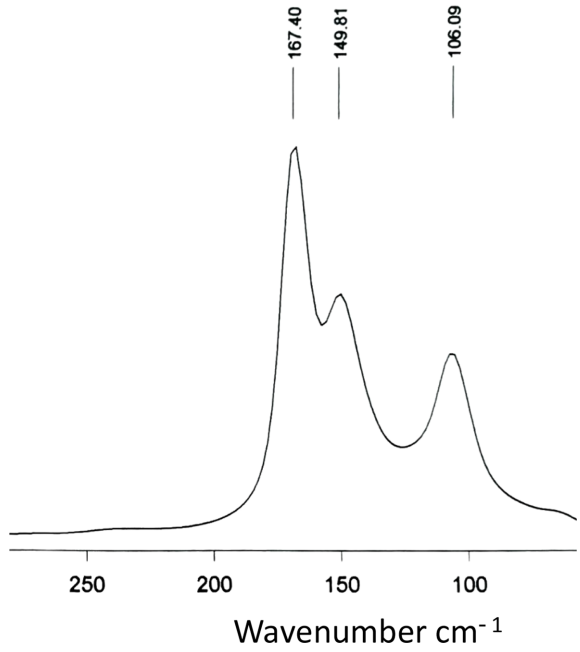

Figure 10
FT–Raman spectrum of (II) in the low frequency region.

and I1—I1^{i} [symmetry code: (i) $-x+2, -y+1, -z$], respectively. These data correspond closely to the established linear correlation ν(I–I)/cm^{-1} *versus* d(I–I)/Å for weak or medium–weak adducts (Arca *et al.*, 2006). The peak at 106 cm^{-1} can be attributed to the symmetric stretch (ν_1) of the I_3^- ion (I2—I3—I4), thus confirming the description of the I_{18}^{4-} polyiodide as an $[(I^-)_2{\cdot}(I_3^-)_2{\cdot}(I_2)_5]$ adduct.

4. Conclusions

In this article, we confirm the structural variety of extended polyiodides that can be generated by changing the shape, charge and dimension of the cation template, as well as the synthetic strategy adopted and the experimental conditions. Although it is still often difficult to characterize $[I_{2m+n}]^{n-}$ polyiodides higher than I_3^- on the grounds of any distinctive structural parameters, such as I—I bond distances, FT–Raman spectroscopy appears to confirm their characterization as aggregates of I_2, I^- and (symmetric or slightly asymmetric) I_3^- building blocks held together by I···I interactions of varying strengths. On the other hand, FT–Raman spectroscopy cannot provide any information on the topological features of extended polyiodides. The two techniques should therefore be used together in the analysis of this kind of compound.

Acknowledgements

We thank Professor Francesco Demartin for useful discussions. We thank the University of Cagliari for financial support and the EPSRC (UK) for the award of X-ray diffractometers.

Data availability

The authors confirm that the data supporting the findings of this study are available within the article and its supplementary materials.

Funding information

The following funding is acknowledged: Engineering and Physical Sciences Research Council (grant Nos. GR/M54728/01 and GR/K45210/01).

References

Aragoni, M. C., Arca, M., Demartin, F., Garau, A., Isaia, F., Lippolis, V. & Pivetta, T. (2023*a*). *New J. Chem.* **47**, 8122–8130.
Aragoni, M. C., Arca, M., Devillanova, F. A., Isaia, F., Lippolis, V., Mancini, A., Pala, L., Slawin, M. Z. & Woollins, J. D. (2003). *Chem. Commun.* pp. 2226–2227.
Aragoni, M. C., Arca, M., Devillanova, V., Hursthouse, M. B., Huth, S. L., Isaia, F., Lippolis, V. & Mancini, A. (2004). *CrystEngComm*, **6**, 540–542.
Aragoni, M. C., Podda, E., Arca, M., Pintus, A., Lippolis, V., Caltagirone, C., Bartz, R. H., Lenardão, E. J., Perin, G., Schumacher, R. F., Coles, S. J. & Orton, J. B. (2022). *New J. Chem.* **46**, 21921–21929.
Aragoni, M. C., Podda, E., Chaudhary, S., Bhasin, A. K. K., Bhasin, K. K., Coles, S. J., Orton, J. B., Isaia, F., Lippolis, V., Pintus, A., Slawin, A. M. Z., Woollins, J. D. & Arca, M. (2023*b*). *Chem. Asian J.* **18**, e202300836.
Arca, M., Aragoni, M. C., Devillanova, F. A., Garau, A., Isaia, F., Lippolis, V., Mancini, A. & Verani, V. (2006). *Bioinorg. Chem. Appl.* **2006**, 1–12.
Arca, M., Demartin, F., Devillanova, F. A., Garau, A., Isaia, F., Lippolis, V. & Verani, G. (1999). *J. Chem. Soc. Dalton Trans.* pp. 3069–3073.
Bigoli, F., Deplano, P., Devillanova, F. A., Lippolis, V., Mercuri, M. L., Pellinghelli, M. A. & Trogu, E. F. (1998). *Inorg. Chim. Acta*, **267**, 115–121.
Blake, A. J., Cristiani, F., Devillanova, F. A., Garau, A., Gilby, L., Gould, R. O., Isaia, F., Lippolis, V., Parsons, S., Radek, C. & Schröder, M. (1997). *J. Chem. Soc. Dalton Trans.* pp. 1337–1346.
Blake, A. J., Gould, R. O., Li, W.-S., Lippolis, V., Parsons, S., Radek, C. & Schröder, M. (1998*a*). *Angew. Chem. Int. Ed. Engl.* **37**, 293–296.
Blake, A. J., Gould, R. O., Li, W.-S., Lippolis, V., Parsons, S., Radek, C. & Schröder, M. (1998*b*). *Inorg. Chem.* **37**, 5070–5077.
Blake, A. J., Li, W., Lippolis, V., Schröder, M., Devillanova, F. O., Gould, R., Parsons, S. & Radek, C. (1998*c*). *Chem. Soc. Rev.* **27**, 195–205.
Blake, A. J., Li, W.-S., Lippolis, V., Parsons, S. & Schröder, M. (1998*d*). *Acta Cryst.* C**54**, 1408–1410.
Blake, A. J., Lippolis, V., Parsons, S. & Schröder, M. (1996). *Chem. Commun.* pp. 2207–2208.
Blake, A. J., Reid, G. & Schröder, M. (1990). *J. Chem. Soc. Dalton Trans.* pp. 3363–3373.
Bruker (2001). *SAINT* and *SADABS*. Bruker AXS Inc., Madison, Wisconsin, USA.
Ciancaleoni, G., Arca, M., Caramori, G. F., Frenking, G., Schneider, F. S. S. & Lippolis, V. (2016). *Eur. J. Inorg. Chem.* **2016**, 3804–3812.
Dolomanov, O. V., Bourhis, L. J., Gildea, R. J., Howard, J. A. K. & Puschmann, H. (2009). *J. Appl. Cryst.* **42**, 339–341.
Fei, Z., Bobbink, F. D., Păunescu, E., Scopelliti, R. & Dyson, P. J. (2015). *Inorg. Chem.* **54**, 10504–10512.
Fiolka, C., Pantenburg, I. & Meyer, G. (2011). *Cryst. Growth Des.* **11**, 5159–5165.
Garau, A., Aragoni, M. C., Arca, M., Caltagirone, C., Demartin, F., Isaia, F., Lippolis, V. & Pivetta, T. (2022). *New J. Chem.* **46**, 6870–6877.
Horn, C. J., Blake, A. J., Champness, N. R., Garau, A., Lippolis, V., Wilson, C. & Schröder, M. (2003*a*). *Chem. Commun.* pp. 312–313.
Horn, C. J., Blake, A. J., Champness, N. R., Lippolis, V. & Schröder, M. (2003*b*). *Chem. Commun.* pp. 1488–1489.
Paulsson, H., Berggrund, M., Svantesson, E., Hagfeldt, A. & Kloo, L. (2004). *Solar Energy Mater. Solar Cells*, **82**, 345–360.
Savastano, M. (2021). *Dalton Trans.* **50**, 7022-7025.
Savastano, M., Bazzicalupi, C. & Bianchi, A. (2022). *Dalton Trans.* **51**, 10728–10739.
Sheldrick, G. M. (1997). *SHELXS97*. University of Göttingen, Germany.
Sheldrick, G. M. (2015*a*). *Acta Cryst.* A**71**, 3–8.
Sheldrick, G. M. (2015*b*). *Acta Cryst.* C**71**, 3–8.
Sonnenberg, K., Mann, L., Redeker, F. A., Schmidt, B. & Riedel, S. (2020). *Angew. Chem. Int. Ed.* **59**, 5464–5493.
Stoe & Cie (1996). *STADI4* and *REDU4*. Stoe & Cie, Darmstadt, Germany.
Svensson, H. & Kloo, L. (2003). *Chem. Rev.* **103**, 1649–1684.
Yin, Z., Wang, Q.-X. & Zeng, M.-H. (2012). *J. Am. Chem. Soc.* **134**, 4857–4863.

supporting information

Acta Cryst. (2024). C**80** [https://doi.org/10.1107/S2053229624004194]

Formation of extended polyiodides at large cation templates

Alexander J. Blake, Carlo Castellano, Vito Lippolis, Enrico Podda and Martin Schröder

Computing details

(*μ*-1,4,10,13-Tetrathia-7,16-diazacyclooctadecane)bis[iodidopalladium(II)] diiodide penta(diiodine) (I)

Crystal data

$[Pd_2I_2(C_{12}H_{26}N_2S_4)](I)_2{\cdot}5I_2$
M_r = 2315.99
Monoclinic, *C*2/*c*
a = 21.609 (4) Å
b = 8.198 (3) Å
c = 24.151 (3) Å
β = 100.170 (13)°
V = 4211.1 (18) Å^3
Z = 4
F(000) = 4040
D_x = 3.653 Mg m^{-3}
Mo *Kα* radiation, *λ* = 0.71073 Å
Cell parameters from 25 reflections
θ = 5–20°
μ = 11.33 mm^{-1}
T = 220 K
Column, red
0.26 × 0.14 × 0.13 mm

Data collection

STOE STADI4 4-circle diffractometer
Scan width (*ω*) = 1.64 – 2.20, scan ratio 2*θ*:*ω* = 1.00 I(Net) and sigma(I) from profile fitting (Clegg, 1981)
Absorption correction: integration (REDU4; Stoe & Cie, 1996)
T_{min} = 0.222, T_{max} = 0.306
4584 measured reflections
3715 independent reflections
3059 reflections with $I > 2\sigma(I)$
R_{int} = 0.029
θ_{max} = 25.0°, θ_{min} = 2.7°
h = −25→25
k = 0→9
l = −28→28
3 standard reflections every 60 reflections
intensity decay: 5.0%

Refinement

Refinement on F^2
Least-squares matrix: full
$R[F^2 > 2\sigma(F^2)]$ = 0.051
$wR(F^2)$ = 0.136
S = 1.08
3715 reflections
163 parameters
0 restraints
Primary atom site location: structure-invariant direct methods
Hydrogen site location: inferred from neighbouring sites
H-atom parameters constrained
$w = 1/[\sigma^2(F_o^2) + (0.0681P)^2 + 91.8532P]$ where $P = (F_o^2 + 2F_c^2)/3$
$(\Delta/\sigma)_{max}$ = 0.001
$\Delta\rho_{max}$ = 1.35 e Å^{-3}
$\Delta\rho_{min}$ = −1.61 e Å^{-3}

Special details

Geometry. All esds (except the esd in the dihedral angle between two l.s. planes) are estimated using the full covariance matrix. The cell esds are taken into account individually in the estimation of esds in distances, angles and torsion angles; correlations between esds in cell parameters are only used when they are defined by crystal symmetry. An approximate (isotropic) treatment of cell esds is used for estimating esds involving l.s. planes.

Refinement. Diffraction data were collected on Stoe STADI4 4-circle and APEXII CCD area detector diffractometers for $[Pd_2I_2([18]aneN_2S_4)](I)_2.(I_2)_5$, (I)< and $[H_2([2.2.2]cryptand)](I_3)(I)(I_2)_{2.5}.CH_2Cl_2$, (II), respectively. The structures were solved by direct methods using *SHELXS* (Sheldrick, 1997) or *SHELXT2018* (Sheldrick, 2015*a*) and developed by iterative cycles of least-squares refinement on F^2 using *SHELXL2018* (Sheldrick, 2015*b*). *OLEX2* (Dolomanov *et al.*, 2009) was used both as the graphical interface for the structural investigation and for the preparation of the figures.

Fractional atomic coordinates and isotropic or equivalent isotropic displacement parameters (Å²)

	x	*y*	*z*	U_{iso}*/U_{eq}	Occ. (<1)
Pd	0.74558 (4)	0.20976 (10)	0.41095 (3)	0.0265 (2)	
I	0.74355 (4)	−0.07058 (10)	0.45843 (3)	0.0396 (2)	
N1	0.7472 (4)	0.4224 (12)	0.3645 (4)	0.033 (2)	
H1	0.745717	0.388974	0.324940	0.039*	
C2	0.6914 (6)	0.5217 (15)	0.3658 (5)	0.036 (3)	
H2A	0.689655	0.611209	0.338668	0.043*	
H2B	0.693364	0.568860	0.403345	0.043*	
C3	0.6334 (5)	0.4162 (15)	0.3512 (4)	0.032 (3)	
H3A	0.628665	0.382092	0.311775	0.039*	
H3B	0.596243	0.480422	0.355395	0.039*	
S4	0.63730 (13)	0.2371 (4)	0.39546 (11)	0.0307 (6)	
C5	0.6221 (5)	0.3303 (14)	0.4610 (4)	0.028 (2)	
H5A	0.654611	0.411792	0.474030	0.034*	
H5B	0.581340	0.385964	0.453828	0.034*	
C6	0.6220 (5)	0.2026 (14)	0.5058 (4)	0.029 (2)	
H6A	0.650767	0.114176	0.500145	0.035*	
H6B	0.579687	0.156393	0.502622	0.035*	
S7	0.64573 (13)	0.2877 (4)	0.57479 (11)	0.0283 (6)	
C8	0.6386 (5)	0.1087 (15)	0.6175 (5)	0.033 (3)	
H8A	0.637648	0.143110	0.656212	0.040*	
H8B	0.598808	0.053577	0.603074	0.040*	
C9	0.6921 (6)	−0.0100 (14)	0.6177 (5)	0.033 (3)	
H9A	0.688681	−0.099724	0.643794	0.040*	
H9B	0.690389	−0.055880	0.580004	0.040*	
I1	0.17411 (5)	0.49110 (13)	0.27632 (4)	0.0541 (3)	
I2	0.30416 (5)	0.44729 (11)	0.29934 (3)	0.0471 (3)	
I3	0.44647 (5)	0.35848 (16)	0.33110 (4)	0.0632 (3)	
I4	0.44322 (4)	0.28503 (11)	0.46091 (4)	0.0498 (3)	
I5	0.45421 (5)	0.21053 (14)	0.57386 (5)	0.0615 (3)	
I6	0.48062 (11)	0.7092 (3)	0.27188 (9)	0.0694 (6)	0.5
I7	0.50658 (10)	1.0005 (3)	0.22248 (9)	0.0692 (6)	0.5

Atomic displacement parameters (Å²)

	U^{11}	U^{22}	U^{33}	U^{12}	U^{13}	U^{23}
Pd	0.0277 (4)	0.0317 (5)	0.0191 (4)	0.0014 (4)	0.0018 (3)	0.0031 (3)
I	0.0446 (5)	0.0385 (5)	0.0356 (4)	0.0007 (4)	0.0066 (3)	0.0056 (3)
N1	0.036 (5)	0.036 (5)	0.025 (5)	0.005 (4)	0.004 (4)	0.007 (4)
C2	0.040 (6)	0.034 (6)	0.032 (6)	0.005 (5)	0.002 (5)	0.011 (5)
C3	0.033 (6)	0.041 (7)	0.021 (5)	0.010 (5)	−0.003 (4)	0.007 (5)
S4	0.0275 (13)	0.0446 (17)	0.0183 (12)	0.0019 (12)	−0.0011 (10)	0.0005 (12)
C5	0.031 (5)	0.034 (6)	0.019 (5)	0.006 (5)	0.005 (4)	0.000 (5)
C6	0.032 (6)	0.038 (6)	0.015 (5)	0.000 (5)	−0.004 (4)	−0.004 (5)
S7	0.0296 (13)	0.0367 (15)	0.0189 (12)	0.0031 (12)	0.0048 (10)	0.0007 (11)
C8	0.030 (6)	0.042 (7)	0.027 (6)	0.000 (5)	0.005 (5)	−0.005 (5)
C9	0.048 (7)	0.027 (6)	0.026 (6)	−0.004 (5)	0.011 (5)	0.000 (5)
I1	0.0707 (6)	0.0609 (6)	0.0275 (4)	0.0073 (5)	−0.0003 (4)	−0.0030 (4)
I2	0.0735 (6)	0.0451 (5)	0.0243 (4)	−0.0062 (4)	0.0128 (4)	−0.0044 (3)
I3	0.0516 (6)	0.0845 (8)	0.0538 (6)	−0.0055 (5)	0.0096 (5)	−0.0075 (5)
I4	0.0310 (4)	0.0478 (5)	0.0666 (6)	0.0020 (4)	−0.0023 (4)	−0.0141 (5)
I5	0.0483 (5)	0.0740 (7)	0.0617 (6)	0.0060 (5)	0.0080 (5)	−0.0112 (5)
I6	0.0612 (12)	0.0961 (17)	0.0465 (11)	0.0254 (12)	−0.0021 (9)	−0.0094 (11)
I7	0.0578 (12)	0.1024 (18)	0.0451 (10)	0.0283 (12)	0.0026 (9)	−0.0041 (11)

Geometric parameters (Å, º)

Pd—I	2.5722 (14)	C5—H5B	0.9800
Pd—N1	2.076 (9)	C5—C6	1.507 (15)
Pd—S4	2.314 (3)	C6—H6A	0.9800
Pd—S7^{i}	2.313 (3)	C6—H6B	0.9800
N1—H1	0.9900	C6—S7	1.796 (10)
N1—C2	1.459 (15)	S7—C8	1.816 (12)
N1—C9^{i}	1.489 (16)	C8—H8A	0.9800
C2—H2A	0.9800	C8—H8B	0.9800
C2—H2B	0.9800	C8—C9	1.511 (16)
C2—C3	1.514 (17)	C9—H9A	0.9800
C3—H3A	0.9800	C9—H9B	0.9800
C3—H3B	0.9800	I1—I2	2.7899 (15)
C3—S4	1.809 (11)	I3—I7^{ii}	3.432 (3)
S4—C5	1.838 (10)	I4—I5	2.7644 (16)
C5—H5A	0.9800	I6—I7	2.771 (4)
N1—Pd—I	173.8 (3)	S4—C5—H5A	109.5
N1—Pd—S4	86.8 (3)	S4—C5—H5B	109.5
N1—Pd—S7^{i}	87.7 (3)	H5A—C5—H5B	108.1
S4—Pd—I	93.57 (8)	C6—C5—S4	110.7 (8)
S7^{i}—Pd—I	92.20 (8)	C6—C5—H5A	109.5
S7^{i}—Pd—S4	173.88 (11)	C6—C5—H5B	109.5
Pd—N1—H1	106.8	C5—C6—H6A	109.4
C2—N1—Pd	111.4 (7)	C5—C6—H6B	109.4

C2—N1—H1	106.8	C5—C6—S7	111.1 (8)
C2—N1—C9^{i}	114.4 (9)	H6A—C6—H6B	108.0
C9^{i}—N1—Pd	110.3 (7)	S7—C6—H6A	109.4
C9^{i}—N1—H1	106.8	S7—C6—H6B	109.4
N1—C2—H2A	109.8	C6—S7—Pd^{i}	104.9 (4)
N1—C2—H2B	109.8	C6—S7—C8	100.0 (5)
N1—C2—C3	109.3 (10)	C8—S7—Pd^{i}	96.2 (4)
H2A—C2—H2B	108.3	S7—C8—H8A	109.1
C3—C2—H2A	109.8	S7—C8—H8B	109.1
C3—C2—H2B	109.8	H8A—C8—H8B	107.9
C2—C3—H3A	109.2	C9—C8—S7	112.4 (8)
C2—C3—H3B	109.2	C9—C8—H8A	109.1
C2—C3—S4	112.1 (7)	C9—C8—H8B	109.1
H3A—C3—H3B	107.9	N1^{i}—C9—C8	109.0 (9)
S4—C3—H3A	109.2	N1^{i}—C9—H9A	109.9
S4—C3—H3B	109.2	N1^{i}—C9—H9B	109.9
C3—S4—Pd	96.6 (4)	C8—C9—H9A	109.9
C3—S4—C5	100.0 (5)	C8—C9—H9B	109.9
C5—S4—Pd	103.3 (4)	H9A—C9—H9B	108.3

Pd—N1—C2—C3	−49.8 (11)	S4—C5—C6—S7	151.6 (6)
Pd—S4—C5—C6	−81.5 (8)	C5—C6—S7—Pd^{i}	−82.2 (8)
Pd^{i}—S7—C8—C9	−30.4 (8)	C5—C6—S7—C8	178.6 (8)
N1—C2—C3—S4	53.8 (11)	C6—S7—C8—C9	76.0 (9)
C2—C3—S4—Pd	−29.9 (9)	S7—C8—C9—N1^{i}	54.5 (11)
C2—C3—S4—C5	74.9 (9)	C9^{i}—N1—C2—C3	−175.8 (9)
C3—S4—C5—C6	179.2 (8)		

Symmetry codes: (i) −*x*+3/2, −*y*+1/2, −*z*+1; (ii) −*x*+1, *y*−1, −*z*+1/2.

4,7,13,16,21,24-Hexaoxa-1,10-diazoniabicyclo[8.8.8]hexacosane triiodide iodide hemipenta(diiodine) dichloromethane monosolvate (II)

Crystal data

$C_{18}H_{38}N_2O_6^{2+}\cdot I_3^-\cdot I^-\cdot 2.5I_2\cdot CH_2Cl_2$	$F(000) = 2908$
$M_r = 1605.53$	$D_x = 2.585$ Mg m^{-3}
Monoclinic, $P2_1/n$	Mo $K\alpha$ radiation, $\lambda = 0.71073$ Å
$a = 13.831$ (2) Å	Cell parameters from 1024 reflections
$b = 14.820$ (2) Å	$\theta = 2.3$–$25.0°$
$c = 20.266$ (3) Å	$\mu = 6.92$ mm^{-1}
$\beta = 96.70$ (1)°	$T = 293$ K
$V = 4125.6$ (10) Å^3	Prism, dark brown
$Z = 4$	0.2 × 0.15 × 0.11 mm

Data collection

Bruker APEXII CCD diffractometer	$T_{min} = 0.569$, $T_{max} = 1.000$
ω scan	30347 measured reflections
Absorption correction: empirical (using intensity measurements) (SADABS; Bruker, 2001)	8100 independent reflections
	5518 reflections with $I > 2\sigma(I)$
	$R_{int} = 0.047$
	$\theta_{max} = 26.0°$, $\theta_{min} = 1.7°$

$h = -17 \rightarrow 17$
$k = -17 \rightarrow 18$
$l = -24 \rightarrow 24$

Refinement

Refinement on F^2
Least-squares matrix: full
$R[F^2 > 2\sigma(F^2)] = 0.033$
$wR(F^2) = 0.088$
$S = 1.00$
8100 reflections
349 parameters
0 restraints
Primary atom site location: dual
Hydrogen site location: mixed
H atoms treated by a mixture of independent and constrained refinement
$w = 1/[\sigma^2(F_o^2) + (0.0409P)^2 + 2.6443P]$ where $P = (F_o^2 + 2F_c^2)/3$
$(\Delta/\sigma)_{max} = 0.002$
$\Delta\rho_{max} = 1.37$ e Å^{-3}
$\Delta\rho_{min} = -1.20$ e Å^{-3}

Special details

Geometry. All esds (except the esd in the dihedral angle between two l.s. planes) are estimated using the full covariance matrix. The cell esds are taken into account individually in the estimation of esds in distances, angles and torsion angles; correlations between esds in cell parameters are only used when they are defined by crystal symmetry. An approximate (isotropic) treatment of cell esds is used for estimating esds involving l.s. planes.

Refinement. Diffraction data were collected on Stoe STADI4 4-circle and APEXII CCD area detector diffractometers for $[Pd_2I_2([18]aneN_2S_4)](I)_2.(I_2)_5$, (I)< and $[H_2([2.2.2]cryptand)](I_3)(I)(I_2)_{2.5}.CH_2Cl_2$, (II), respectively. The structures were solved by direct methods using *SHELXS* (Sheldrick, 1997) or *SHELXT2018* (Sheldrick, 2015*a*) and developed by iterative cycles of least-squares refinement on F^2 using *SHELXL2018* (Sheldrick, 2015*b*). *OLEX2* (Dolomanov *et al.*, 2009) was used both as the graphical interface for the structural investigation and for the preparation of the figures.

Fractional atomic coordinates and isotropic or equivalent isotropic displacement parameters (Å²)

	x	*y*	*z*	U_{iso}*/U_{eq}
I3	0.97532 (3)	0.09815 (3)	−0.09154 (2)	0.05246 (13)
I6	1.18118 (3)	0.25227 (3)	0.29099 (2)	0.05446 (13)
I8	1.02564 (4)	0.12201 (3)	0.44048 (2)	0.05614 (13)
I1	1.04190 (4)	0.41593 (4)	−0.00367 (2)	0.06090 (14)
I5	1.14617 (4)	0.36573 (4)	0.18021 (3)	0.06725 (15)
I9	0.84017 (4)	0.12912 (4)	0.48279 (3)	0.07124 (16)
I2	1.11920 (4)	0.19711 (4)	0.00283 (3)	0.07161 (16)
I4	0.84421 (4)	−0.00647 (4)	−0.18076 (3)	0.07345 (17)
I7	1.23723 (4)	0.11657 (4)	0.40516 (3)	0.08026 (18)
Cl1	0.95495 (16)	0.38674 (16)	0.32137 (13)	0.0828 (6)
Cl2	0.7726 (2)	0.39206 (15)	0.37582 (16)	0.1031 (9)
O3	1.0138 (3)	0.5948 (3)	0.4173 (2)	0.0507 (11)
O4	0.8153 (3)	0.6262 (3)	0.4468 (2)	0.0505 (11)
O6	0.7318 (3)	0.8559 (3)	0.3468 (2)	0.0572 (12)
O5	0.9379 (3)	0.8313 (3)	0.3301 (2)	0.0546 (12)
O2	0.8968 (3)	0.6260 (3)	0.2316 (2)	0.0557 (12)
O1	0.7020 (3)	0.6014 (3)	0.2611 (2)	0.0571 (12)
N2	1.0574 (4)	0.6895 (4)	0.3026 (3)	0.0418 (12)
H2	1.001 (5)	0.686 (4)	0.314 (3)	0.050*
N1	0.6452 (4)	0.6877 (3)	0.3760 (3)	0.0413 (12)
H1	0.699 (5)	0.691 (4)	0.362 (3)	0.050*
C11	0.7283 (5)	0.6077 (5)	0.4753 (4)	0.0549 (18)
H11A	0.716852	0.654111	0.507249	0.066*

H11B	0.733234	0.549923	0.497966	0.066*
C7	1.1296 (4)	0.6832 (4)	0.3634 (3)	0.0473 (16)
H7A	1.125640	0.737570	0.389610	0.057*
H7B	1.194607	0.680113	0.350046	0.057*
C9	0.9878 (5)	0.6552 (5)	0.4663 (4)	0.0548 (18)
H9A	0.975004	0.714386	0.446738	0.066*
H9B	1.041407	0.660797	0.501438	0.066*
C2	0.6032 (5)	0.6010 (5)	0.2706 (4)	0.0609 (19)
H2A	0.587977	0.544205	0.290791	0.073*
H2B	0.564287	0.604898	0.227653	0.073*
C15	0.8113 (5)	0.8730 (5)	0.3951 (4)	0.0540 (17)
H15A	0.827712	0.818663	0.420665	0.065*
H15B	0.793995	0.919471	0.425342	0.065*
C8	1.1135 (5)	0.6028 (5)	0.4057 (4)	0.0542 (18)
H8A	1.132992	0.548567	0.383870	0.065*
H8B	1.154018	0.608160	0.447929	0.065*
C12	0.6466 (5)	0.6061 (4)	0.4194 (4)	0.0549 (18)
H12A	0.653090	0.552702	0.392511	0.066*
H12B	0.585150	0.601838	0.437805	0.066*
C4	0.8137 (5)	0.6384 (6)	0.1838 (3)	0.062 (2)
H4A	0.797239	0.581965	0.161018	0.074*
H4B	0.828128	0.682662	0.151120	0.074*
C6	1.0670 (5)	0.6125 (5)	0.2557 (4)	0.0565 (18)
H6A	1.069183	0.556145	0.280203	0.068*
H6B	1.127538	0.618509	0.236363	0.068*
C17	1.0294 (5)	0.8552 (5)	0.3096 (4)	0.061 (2)
H17A	1.077173	0.864245	0.348067	0.073*
H17B	1.023659	0.910587	0.284027	0.073*
C13	0.6242 (5)	0.7734 (4)	0.4118 (4)	0.0523 (17)
H13A	0.557033	0.772228	0.421256	0.063*
H13B	0.665384	0.775461	0.453878	0.063*
C18	1.0600 (5)	0.7792 (5)	0.2680 (4)	0.061 (2)
H18A	1.125533	0.790410	0.257413	0.073*
H18B	1.017123	0.777002	0.226584	0.073*
C16	0.8968 (5)	0.9029 (5)	0.3625 (4)	0.0578 (19)
H16A	0.876653	0.949941	0.330521	0.069*
H16B	0.945446	0.928241	0.395730	0.069*
C3	0.7294 (5)	0.6700 (5)	0.2179 (4)	0.0590 (19)
H3A	0.747298	0.724232	0.243136	0.071*
H3B	0.674802	0.684256	0.184983	0.071*
C10	0.8991 (5)	0.6225 (5)	0.4950 (3)	0.0553 (18)
H10A	0.909439	0.560824	0.510303	0.066*
H10B	0.888319	0.659487	0.532918	0.066*
C5	0.9834 (5)	0.6101 (6)	0.2012 (4)	0.062 (2)
H5A	0.991440	0.656283	0.168403	0.074*
H5B	0.980229	0.551744	0.179350	0.074*
C14	0.6405 (5)	0.8573 (5)	0.3732 (4)	0.061 (2)
H14A	0.588429	0.863464	0.337011	0.074*

H14B	0.638214	0.909355	0.402005	0.074*
C1	0.5754 (5)	0.6783 (5)	0.3143 (4)	0.0563 (18)
H1A	0.574059	0.734240	0.289300	0.068*
H1B	0.510513	0.667798	0.326374	0.068*
C19	0.8493 (6)	0.4487 (6)	0.3270 (5)	0.080 (3)
H19A	0.815558	0.458231	0.282869	0.096*
H19B	0.866206	0.507217	0.346411	0.096*

Atomic displacement parameters (Å²)

	U^{11}	U^{22}	U^{33}	U^{12}	U^{13}	U^{23}
I3	0.0500 (3)	0.0529 (3)	0.0579 (3)	0.0116 (2)	0.0208 (2)	0.0112 (2)
I6	0.0374 (2)	0.0686 (3)	0.0589 (3)	−0.0009 (2)	0.0123 (2)	−0.0057 (2)
I8	0.0663 (3)	0.0498 (3)	0.0490 (3)	0.0015 (2)	−0.0071 (2)	−0.0035 (2)
I1	0.0563 (3)	0.0793 (3)	0.0488 (3)	−0.0036 (2)	0.0133 (2)	0.0120 (2)
I5	0.0550 (3)	0.0809 (4)	0.0649 (3)	0.0043 (3)	0.0032 (2)	0.0090 (3)
I9	0.0566 (3)	0.0829 (4)	0.0709 (4)	0.0029 (3)	−0.0070 (3)	−0.0118 (3)
I2	0.0556 (3)	0.0782 (4)	0.0817 (4)	0.0073 (3)	0.0109 (3)	−0.0141 (3)
I4	0.0570 (3)	0.0763 (4)	0.0870 (4)	−0.0116 (3)	0.0080 (3)	0.0080 (3)
I7	0.0750 (4)	0.0988 (4)	0.0689 (4)	0.0195 (3)	0.0168 (3)	0.0200 (3)
Cl1	0.0651 (12)	0.0855 (15)	0.1010 (17)	0.0109 (11)	0.0239 (12)	−0.0196 (13)
Cl2	0.1055 (19)	0.0674 (14)	0.152 (3)	−0.0064 (13)	0.0815 (19)	−0.0079 (14)
O3	0.041 (2)	0.059 (3)	0.053 (3)	−0.004 (2)	0.008 (2)	−0.005 (2)
O4	0.039 (2)	0.067 (3)	0.046 (3)	0.003 (2)	0.009 (2)	0.006 (2)
O6	0.046 (3)	0.067 (3)	0.062 (3)	−0.010 (2)	0.017 (2)	−0.011 (2)
O5	0.045 (3)	0.051 (3)	0.072 (3)	−0.001 (2)	0.025 (2)	−0.004 (2)
O2	0.042 (3)	0.085 (4)	0.039 (3)	0.001 (2)	0.003 (2)	0.000 (2)
O1	0.048 (3)	0.067 (3)	0.057 (3)	0.012 (2)	0.010 (2)	0.000 (2)
N2	0.026 (2)	0.053 (3)	0.048 (3)	0.005 (2)	0.016 (2)	0.007 (3)
N1	0.033 (3)	0.038 (3)	0.056 (3)	−0.005 (2)	0.014 (2)	−0.011 (2)
C11	0.054 (4)	0.062 (4)	0.053 (4)	−0.002 (3)	0.023 (3)	0.008 (3)
C7	0.030 (3)	0.058 (4)	0.053 (4)	−0.003 (3)	0.004 (3)	0.007 (3)
C9	0.047 (4)	0.057 (4)	0.060 (5)	−0.006 (3)	0.000 (3)	−0.002 (4)
C2	0.049 (4)	0.077 (5)	0.056 (5)	−0.008 (4)	0.005 (3)	−0.017 (4)
C15	0.044 (4)	0.064 (4)	0.055 (4)	0.000 (3)	0.008 (3)	−0.008 (4)
C8	0.038 (4)	0.066 (5)	0.060 (5)	0.008 (3)	0.014 (3)	0.011 (4)
C12	0.048 (4)	0.046 (4)	0.075 (5)	−0.005 (3)	0.024 (4)	−0.005 (4)
C4	0.050 (4)	0.096 (6)	0.039 (4)	0.002 (4)	0.001 (3)	0.001 (4)
C6	0.047 (4)	0.064 (5)	0.061 (5)	0.003 (3)	0.017 (3)	−0.008 (4)
C17	0.060 (4)	0.044 (4)	0.085 (6)	−0.004 (3)	0.031 (4)	0.013 (4)
C13	0.050 (4)	0.047 (4)	0.065 (5)	−0.003 (3)	0.028 (3)	−0.015 (3)
C18	0.051 (4)	0.069 (5)	0.066 (5)	0.012 (4)	0.027 (4)	0.028 (4)
C16	0.051 (4)	0.043 (4)	0.080 (5)	−0.007 (3)	0.011 (4)	−0.003 (4)
C3	0.053 (4)	0.067 (5)	0.056 (5)	0.009 (4)	0.005 (3)	0.006 (4)
C10	0.056 (4)	0.067 (5)	0.044 (4)	0.003 (4)	0.011 (3)	0.006 (3)
C5	0.054 (4)	0.084 (6)	0.049 (4)	0.002 (4)	0.009 (3)	−0.005 (4)
C14	0.048 (4)	0.045 (4)	0.095 (6)	0.000 (3)	0.023 (4)	−0.011 (4)
C1	0.037 (3)	0.061 (4)	0.069 (5)	0.004 (3)	0.002 (3)	−0.016 (4)

C19	0.068 (5)	0.072 (5)	0.106 (7)	0.020 (4)	0.040 (5)	0.022 (5)

Geometric parameters (Å, º)

I3—I2	2.9799 (8)	C2—H2A	0.9700
I3—I4	2.8629 (8)	C2—H2B	0.9700
I6—I5	2.8015 (8)	C2—C1	1.525 (9)
I6—I7	3.0952 (8)	C15—H15A	0.9700
I8—I9	2.8001 (8)	C15—H15B	0.9700
I8—I7	3.0940 (9)	C15—C16	1.487 (10)
I1—I1^{i}	2.7595 (11)	C8—H8A	0.9700
Cl1—C19	1.741 (8)	C8—H8B	0.9700
Cl2—C19	1.747 (8)	C12—H12A	0.9700
O3—C9	1.415 (8)	C12—H12B	0.9700
O3—C8	1.431 (8)	C4—H4A	0.9700
O4—C11	1.421 (8)	C4—H4B	0.9700
O4—C10	1.428 (8)	C4—C3	1.497 (10)
O6—C15	1.408 (8)	C6—H6A	0.9700
O6—C14	1.429 (8)	C6—H6B	0.9700
O5—C17	1.421 (8)	C6—C5	1.503 (10)
O5—C16	1.403 (8)	C17—H17A	0.9700
O2—C4	1.426 (8)	C17—H17B	0.9700
O2—C5	1.430 (8)	C17—C18	1.497 (10)
O1—C2	1.402 (8)	C13—H13A	0.9700
O1—C3	1.422 (8)	C13—H13B	0.9700
N2—H2	0.84 (7)	C13—C14	1.500 (10)
N2—C7	1.495 (8)	C18—H18A	0.9700
N2—C6	1.500 (8)	C18—H18B	0.9700
N2—C18	1.506 (8)	C16—H16A	0.9700
N1—H1	0.83 (7)	C16—H16B	0.9700
N1—C12	1.493 (8)	C3—H3A	0.9700
N1—C13	1.507 (8)	C3—H3B	0.9700
N1—C1	1.495 (9)	C10—H10A	0.9700
C11—H11A	0.9700	C10—H10B	0.9700
C11—H11B	0.9700	C5—H5A	0.9700
C11—C12	1.505 (10)	C5—H5B	0.9700
C7—H7A	0.9700	C14—H14A	0.9700
C7—H7B	0.9700	C14—H14B	0.9700
C7—C8	1.500 (9)	C1—H1A	0.9700
C9—H9A	0.9700	C1—H1B	0.9700
C9—H9B	0.9700	C19—H19A	0.9700
C9—C10	1.497 (9)	C19—H19B	0.9700
I4—I3—I2	176.54 (2)	C3—C4—H4A	109.7
I5—I6—I7	173.63 (2)	C3—C4—H4B	109.7
I9—I8—I7	175.52 (2)	N2—C6—H6A	109.3
I8—I7—I6	89.70 (2)	N2—C6—H6B	109.3
C9—O3—C8	113.1 (5)	N2—C6—C5	111.5 (6)

C11—O4—C10	111.8 (5)	H6A—C6—H6B	108.0
C15—O6—C14	113.0 (6)	C5—C6—H6A	109.3
C16—O5—C17	111.9 (5)	C5—C6—H6B	109.3
C4—O2—C5	112.2 (5)	O5—C17—H17A	110.3
C2—O1—C3	114.9 (5)	O5—C17—H17B	110.3
C7—N2—H2	110 (5)	O5—C17—C18	107.3 (6)
C7—N2—C6	112.0 (5)	H17A—C17—H17B	108.5
C7—N2—C18	112.9 (5)	C18—C17—H17A	110.3
C6—N2—H2	106 (4)	C18—C17—H17B	110.3
C6—N2—C18	111.6 (6)	N1—C13—H13A	108.9
C18—N2—H2	104 (4)	N1—C13—H13B	108.9
C12—N1—H1	108 (5)	H13A—C13—H13B	107.7
C12—N1—C13	113.0 (5)	C14—C13—N1	113.6 (6)
C12—N1—C1	112.4 (5)	C14—C13—H13A	108.9
C13—N1—H1	111 (5)	C14—C13—H13B	108.9
C1—N1—H1	103 (5)	N2—C18—H18A	109.2
C1—N1—C13	109.8 (5)	N2—C18—H18B	109.2
O4—C11—H11A	110.3	C17—C18—N2	112.2 (6)
O4—C11—H11B	110.3	C17—C18—H18A	109.2
O4—C11—C12	107.0 (6)	C17—C18—H18B	109.2
H11A—C11—H11B	108.6	H18A—C18—H18B	107.9
C12—C11—H11A	110.3	O5—C16—C15	111.7 (6)
C12—C11—H11B	110.3	O5—C16—H16A	109.3
N2—C7—H7A	109.0	O5—C16—H16B	109.3
N2—C7—H7B	109.0	C15—C16—H16A	109.3
N2—C7—C8	113.0 (5)	C15—C16—H16B	109.3
H7A—C7—H7B	107.8	H16A—C16—H16B	107.9
C8—C7—H7A	109.0	O1—C3—C4	109.7 (6)
C8—C7—H7B	109.0	O1—C3—H3A	109.7
O3—C9—H9A	109.5	O1—C3—H3B	109.7
O3—C9—H9B	109.5	C4—C3—H3A	109.7
O3—C9—C10	110.7 (6)	C4—C3—H3B	109.7
H9A—C9—H9B	108.1	H3A—C3—H3B	108.2
C10—C9—H9A	109.5	O4—C10—C9	111.0 (5)
C10—C9—H9B	109.5	O4—C10—H10A	109.4
O1—C2—H2A	108.9	O4—C10—H10B	109.4
O1—C2—H2B	108.9	C9—C10—H10A	109.4
O1—C2—C1	113.1 (6)	C9—C10—H10B	109.4
H2A—C2—H2B	107.8	H10A—C10—H10B	108.0
C1—C2—H2A	108.9	O2—C5—C6	106.9 (6)
C1—C2—H2B	108.9	O2—C5—H5A	110.3
O6—C15—H15A	109.7	O2—C5—H5B	110.3
O6—C15—H15B	109.7	C6—C5—H5A	110.3
O6—C15—C16	110.0 (6)	C6—C5—H5B	110.3
H15A—C15—H15B	108.2	H5A—C5—H5B	108.6
C16—C15—H15A	109.7	O6—C14—C13	112.1 (6)
C16—C15—H15B	109.7	O6—C14—H14A	109.2
O3—C8—C7	111.7 (5)	O6—C14—H14B	109.2

O3—C8—H8A	109.3	C13—C14—H14A	109.2
O3—C8—H8B	109.3	C13—C14—H14B	109.2
C7—C8—H8A	109.3	H14A—C14—H14B	107.9
C7—C8—H8B	109.3	N1—C1—C2	111.9 (5)
H8A—C8—H8B	107.9	N1—C1—H1A	109.2
N1—C12—C11	112.8 (5)	N1—C1—H1B	109.2
N1—C12—H12A	109.0	C2—C1—H1A	109.2
N1—C12—H12B	109.0	C2—C1—H1B	109.2
C11—C12—H12A	109.0	H1A—C1—H1B	107.9
C11—C12—H12B	109.0	Cl1—C19—Cl2	110.7 (5)
H12A—C12—H12B	107.8	Cl1—C19—H19A	109.5
O2—C4—H4A	109.7	Cl1—C19—H19B	109.5
O2—C4—H4B	109.7	Cl2—C19—H19A	109.5
O2—C4—C3	109.7 (6)	Cl2—C19—H19B	109.5
H4A—C4—H4B	108.2	H19A—C19—H19B	108.1

O3—C9—C10—O4	−67.8 (7)	C12—N1—C1—C2	−62.5 (8)
O4—C11—C12—N1	−51.0 (7)	C4—O2—C5—C6	171.4 (6)
O6—C15—C16—O5	−72.6 (8)	C6—N2—C7—C8	−65.1 (7)
O5—C17—C18—N2	−52.5 (8)	C6—N2—C18—C17	167.7 (6)
O2—C4—C3—O1	−65.1 (8)	C17—O5—C16—C15	−169.0 (6)
O1—C2—C1—N1	−47.5 (9)	C13—N1—C12—C11	−65.1 (7)
N2—C7—C8—O3	−48.4 (8)	C13—N1—C1—C2	170.9 (6)
N2—C6—C5—O2	−43.6 (8)	C18—N2—C7—C8	167.9 (5)
N1—C13—C14—O6	−47.8 (9)	C18—N2—C6—C5	−62.6 (7)
C11—O4—C10—C9	−171.7 (6)	C16—O5—C17—C18	−172.5 (6)
C7—N2—C6—C5	169.8 (6)	C3—O1—C2—C1	−73.2 (8)
C7—N2—C18—C17	−65.1 (7)	C10—O4—C11—C12	−175.5 (6)
C9—O3—C8—C7	−77.9 (7)	C5—O2—C4—C3	−170.5 (6)
C2—O1—C3—C4	−150.6 (6)	C14—O6—C15—C16	−159.8 (6)
C15—O6—C14—C13	−75.9 (8)	C1—N1—C12—C11	170.0 (5)
C8—O3—C9—C10	−158.4 (5)	C1—N1—C13—C14	−64.4 (7)
C12—N1—C13—C14	169.3 (6)		

Symmetry code: (i) −*x*+2, −*y*+1, −*z*.